East European Journal of Physics. 4. 328-339 (2025)
DOI:10.26565/2312-4334-2025-4-31 ISSN 2312-4334

PERISTALTIC BILE FLOW IN PAPILLA AMPOULE OF POROUS WALLS AND INCLINED ECCENTRIC CATHETERIZED DUCT

D. Kumar[1]*, T.K. Rawat[2], M. Garvandha[1], S. Kumar[3], S.K. Chaubey[1]
[1]*Sciences and Mathematics Unit, Department of Supportive Requirements, University of Technology and Applied Sciences-Shinas, Oman*
[2]*GLA University, Greater Noida, India*
[3]*Dr. Bhimrao Ambedkar University, Agra, India*
**Corresponding Author e-mail: devendra.kumar@utas.edu.om*
Received September 1, 2025; revised October 4, 2025; accepted October 10, 2025

In this study, the combined effects of inclination and catheter on the biliary flow of a Carreau fluid through an eccentric catheterized duct with a porous material are mathematically investigated. The perturbation technique is employed to solve the governing equations, considering low Reynolds numbers, a long-wavelength approximation, and suitable small parameters. The surgical technique, when a catheter is inserted eccentrically into the duct, is connected to the outcomes of the investigation. Several parameters have been used to achieve the analytical solutions. Axial velocity, pressure gradient, flow rate, and wall shear stress are displayed in these data, together with the following emergent parameters: wall slip parameter, Weissenberg number, fluid behavior index, Darcy number, and angle of inclination. The pressure gradient is significantly altered by the angle of inclination and porosity parameter, and the catheter's axial velocity falls as the Weissenberg number rises. The physiological observations are consistent with these findings.
Keywords: *Peristaltic bile flow; Papilla Ampoule; Porous Walls; Inclined Eccentric Catheterized Duct*
PACS: 02.30.Jr, 02.30.Mv, 47.56.+r, 47.63.-b

INTRODUCTION

The particular kind of pumping called peristaltic pumping makes it simple to move a range of rheological biofluids from one organ to another. The progressive wave of the duct wall's periodic contraction or relaxation causes the peristaltic motion. The catheter is essentially a long tube that is intended for use in ophthalmic, neurological, urological, cardiovascular, and gastrointestinal purposes. In addition to measuring several physiological flow characteristics like flow velocity, flow rate, pressure increase, and pressure gradient, the catheter is employed in clinical procedures to diagnose and treat illnesses. The initial hemodynamic conditions within the duct are disturbed when the catheter is introduced because it causes an annular zone to form between the catheter and the duct wall. Additionally, the catheter increased the flow's frictional resistance. Strasberg *et al*. [13] tested the accuracy of the results of the mathematical model by an experimental investigation. They establish the connection between biliary flow and canalicular clearing. Additionally, the treatment of post-operative bile fistulas by internal endoscopic biliary drainage was investigated by Sauerbruch *et al*. [12]. James *et al*. [4] investigated orthotopic liver transplant recipients who had nasobiliary catheters inserted endoscopically, which aid in rerouting the flow of bile. According to Tripathi *et al*. [14], peristaltic transport via a finite channel, peristaltic heat flow creates a porous environment with greater resistance and enhanced as the Grashof number rises. By observing the effect of Weissenberg number and power index on axial velocity, Nadeem *et al*. [8] studied the unsteady peristaltic transport of Carreau fluid flow in an eccentric tube. It found that the axial velocity profile decreases as the values of the Weissenberg number and the power index increase. According to another mathematical model of papillary stenosis with stone developed by Kuchumov *et al*. [5], the permeability parameter, Weissenberg number, and amplitude ratio all affect the pressure that corresponds to the reflux state. Gudekote *et al*. [3] examined the Casson fluid moving through porous walls impacted by the wall slip parameter and elasticity. They discovered a correlation between rises in pressure and angle of inclination, noting that as the degree of inclination increases, so does the pressure. Nabil *et al*. [7] investigated the impact of heat and mass transfer on Casson fluid flow via two coaxial cylindrical tubes with peristalsis. Nurulaifa *et al*. [9] developed a mathematical model of Bingham fluid flow through an overlapping stenosed artery and discovered that when the plug core radius increased, the dispersion function decreased. It accounts for various leakage instances, such as leaking from the common bile duct lesion, choledochotomy, and cystic duct stump. The viscous flow between two sinusoidal deforming concentric tubes was analytically examined by McCash *et al*. [6]. It also discussed the applications, such as endoscopy of curved human organs and the maintenance and enhancement of intricately designed machinery. Moreover, by using a mathematical model of blood flow through a stenosed artery with post-stenotic dilatation, Dhange *et al*. [2] examined various physical attributes that affect fluid resistance to flow and noted that the surface shearing stress decreased with the upsurge of resistance. Moreover, a mathematical model of an eccentric catheterized artery with heat transfer was studied by Reima *et al*. [11]. They investigated the impact of temperature in the scenario where the artery is the outer tube, and the catheter is the inner tube. The results obtained are consistent with physiological observations as well as the causes and complications related to catheterization. They described how the model is applied to the

Cite as: D. Kumar, T.K. Rawat, M. Garvandha, S. Kumar, S.K. Chaubey, East Eur. J. Phys. 4, 328 (2025), https://doi.org/10.26565/2312-4334-2025-4-31

cardiovascular system and found that the viscosity of the peripheral layer reduces as the wall shear stress lowers. In the investigation of the fractional Oldroyd-B fluid between two coaxial cylinders loaded with gold nanoparticles, Cao *et al*. [1] observed that the inclusion of nanoparticles increased the base fluid's heat capacity. A model of nanolayer fluid flow over a porous surface in the presence of carbon nanotubes was proposed mathematically by Raza *et al*. [10]. They also examined the impact of increasing interfacial nanolayer thickness from 3 to 9 nm, which has a substantial effect on thermal performance and thermal conductivity.

Modern literature shows that bile is not strictly Newtonian: it commonly exhibits shear-thinning and viscoelastic features that vary with bile composition, pathology, and shear-rate range. We therefore justify the Carreau (shear-thinning). Experimental and review studies report shear thinning and viscoelastic features in bile depending on composition and disease state; thus, a shear rate-dependent viscosity model is appropriate for theoretical investigation. Recent reviews summarizing bile rheology, such as those by Kuchumov et al. [5], consider bile as a non-Newtonian fluid. These studies, along with related experimental reports, led to the selection of bile as a Carreau-type model.

In the present study, the combined effects of eccentric tubes, porosity, and angle of inclination on the peristaltic transport of Carreau fluid in an axisymmetric tube were examined. The findings might be beneficial in the various practical applications of medical science. The regular perturbation technique is used to solve the two-dimensional mathematical model in a cylindrical coordinate system. The Weissenberg number and eccentric parameter are involved in the solution of this investigation process. The resulting equations were solved analytically under the appropriate boundary conditions. With the help of influencing factors like the fluid behavior index, amplitude ratio, Darcy number, slip parameter, and angle of inclination, the expression has been derived for axial velocity, pressure gradient, wall shear stress, and flow rate. The obtained expressions were graphically represented in various combinations with emerging parameters. The results of the current model were evaluated and related to the intricate physiological flow of the bile through the diseased duct. It greatly aids in the investigation of bile flow in the duct in a much better way than earlier, especially in dialysis cases.

MATHEMATICAL INTERPRETATION OF THE PROBLEM

The flow of bile is modeled by considering the peristaltic flow of an incompressible Carreau fluid flowing inside the eccentric tubes, in which the inner tube is uniform and rigid, representing a catheter placed in an eccentric position within the pancreatic duct. The pancreatic duct is filled with the porous medium of finite length L and inclined at an angle α with the horizontal is taken into account as the outer tube. The relevant equations of momentum and continuity in vector form are as follows.

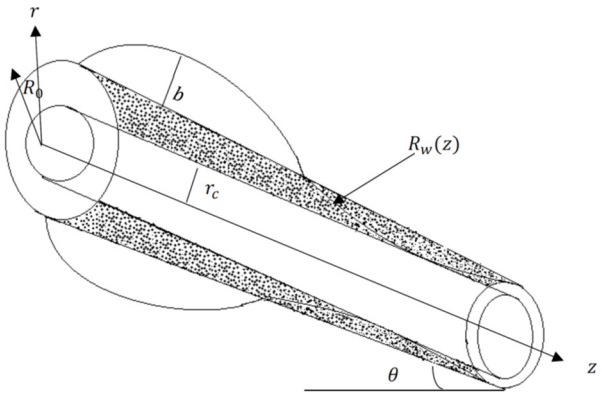

Figure 1. Geometrical representation of the problem

The fluid density ρ is uniform incompressibility conditions, the equation of continuity is:

$$\nabla . V = 0 \tag{1a}$$

The equation governing the motion is:

$$\left(\frac{\partial V}{\partial t} + (\nabla . V)V\right) = -\frac{1}{\rho}\nabla P + \frac{1}{\rho}\nabla . \tau_{ln} \tag{1b}$$

Where, $V = (u, v, w)$, the velocity components in the $r, \theta \; and \; z$ directions respectively, P is the pressure, ρ is the density and τ_{ln} is the extra stress tensor.

The geometry of the non-uniform pancreatic duct with a catheter and the wall deformation due to an infinite sinusoidal wave propagating along the wall is mathematically described as

$$R_w(z) = R_o - mz + ztan\alpha + bsin\frac{2\pi z}{\lambda} \tag{2a}$$

$$R_c(z) = r_c \tag{2b}$$

The constitutive equations for the non-Newtonian fluid are described by the Carreau equation

$$\check{C}_{ln} = -p\delta_{lm} + \check{\tau}_{ln} \tag{3a}$$

$$\check{\tau}_{ln} = \left[\mu_\infty + (\mu_0 - \mu_\infty)(1 + ((\Gamma\check{\bar{\gamma}})^2)^{\frac{m-1}{2}})\right]\check{\bar{\gamma}} \tag{3b}$$

here $\check{\tau}_{ln}$ is the extra stress tensor, p stands for pressure, δ_{ln} is the Kronecker delta, μ_0 and μ_∞ are the zero and infinite shear rate viscosities, Γ is the time constant, and m is the dimensionless fluid behavior index. The shear rate $\bar{\dot{\gamma}}$ is defined as follows:

$$\check{\bar{\gamma}} = \sqrt{\frac{1}{2}\sum\sum\check{\bar{\gamma}}_{ln}\check{\bar{\gamma}}_{nl}} = \sqrt{\frac{1}{2}\Pi} \tag{3c}$$

Where, π is the second invariant strain rate tensor. In case of $\mu_\infty = 0$ and by using Taylor's expansion in equation (3c), we get:

$$\check{\tau}_{ln} = \mu_0\left[1 + \frac{m-1}{2}\left((\Gamma\check{\bar{\gamma}}_{ln})^2\right)\right]\check{\bar{\gamma}}_{ln} \tag{3d}$$

The biliary system, having stenosis, is assumed as a cylindrical elastic tube/model of the circular cross section containing an incompressible non-Newtonian fluid. The bile flow is modeled to be laminar, unsteady, two-dimensional, axially symmetric, and fully developed bile characterized by generalized Carreau model by considering an inclined non-uniform pancreatic duct filled with a porous medium. Under the assumptions, the governing equation may be written in the cylindrical coordinate system $(\check{r}, \check{z}, \check{\theta})$ as

$$\frac{\partial\check{u}}{\partial\check{r}} + \frac{\check{u}}{\check{r}} + \frac{1}{\check{r}}\frac{\partial\check{v}}{\partial\check{\theta}} + \frac{\partial\check{w}}{\partial\check{z}} = 0 \tag{4a}$$

$$\rho\left(\frac{\partial\check{u}}{\partial\check{t}} + \check{u}\frac{\partial\check{u}}{\partial\check{r}} + \frac{\check{v}}{\check{r}}\frac{\partial\check{u}}{\partial\check{\theta}} - \frac{\check{v}^2}{\check{r}} + \check{w}\frac{\partial\check{u}}{\partial\check{z}}\right) = -\frac{\partial\check{p}}{\partial\check{r}} + \frac{1}{\check{r}}\frac{\partial}{\partial\check{r}}(\check{r}\check{C}_{rr}) + \frac{1}{\check{r}}\frac{\partial}{\partial\check{\theta}}(\check{C}_{r\theta}) + \frac{\partial}{\partial\check{z}}\check{C}_{rz} - \frac{\check{C}_{\theta\theta}}{\check{r}} - \rho g\cos\alpha \tag{4b}$$

$$\rho\left(\frac{\partial\check{v}}{\partial\check{t}} + \check{u}\frac{\partial\check{v}}{\partial\check{r}} + \frac{\check{v}}{\check{r}}\frac{\partial\check{v}}{\partial\check{\theta}} + \frac{\check{u}\check{v}}{\check{r}} + \check{w}\frac{\partial\check{v}}{\partial\check{z}}\right) = -\frac{1}{\check{r}}\frac{\partial\check{p}}{\partial\check{\theta}} + \frac{1}{\check{r}^2}\frac{\partial}{\partial\check{r}}(\check{r}^2\check{C}_{r\theta}) + \frac{1}{\check{r}}\frac{\partial}{\partial\check{\theta}}(\check{C}_{\theta\theta}) + \frac{\partial}{\partial\check{z}}\check{C}_{\theta z} \tag{4c}$$

$$\rho\left(\frac{\partial\check{w}}{\partial\check{t}} + \check{u}\frac{\partial\check{w}}{\partial\check{r}} + \frac{\check{v}}{\check{r}}\frac{\partial\check{w}}{\partial\check{\theta}} + \check{w}\frac{\partial\check{w}}{\partial\check{z}}\right) = -\frac{\partial\check{p}}{\partial\check{z}} + \frac{1}{\check{r}}\frac{\partial}{\partial\check{r}}(\check{r}\check{C}_{rz}) + \frac{1}{\check{r}}\frac{\partial}{\partial\check{\theta}}(\check{C}_{\theta z}) + \frac{\partial}{\partial\check{z}}\check{C}_{zz} + \rho g\sin\alpha \tag{4d}$$

Here, ρ stands for density, $\check{w}$ *and* $\check{u}$ are the velocity components, $\check{p}$ is the pressure, $\sigma^2 = \frac{\epsilon}{Da}$, $Da = \frac{k}{a^2}$, ∈ is porosity, k is the permeability, and Da is the Darcy number.
From equation (3a) - (3c) and (3d) we get:

$$\frac{1}{2}\check{\bar{\gamma}}\check{\bar{\gamma}} = 2\left\{\left(\frac{\partial\check{w}}{\partial\check{r}}\right)^2 + \left(\frac{\check{w}}{\check{r}}\right)^2 + \left(\frac{\partial\check{u}}{\partial\check{z}}\right)^2\right\} + \left(\frac{\partial\check{w}}{\partial\check{z}} + \frac{\partial\check{u}}{\partial\check{r}}\right)^2, \tag{5a}$$

$$\check{C}_{rr} = 2\mu_0\left[1 + \frac{m-1}{2}\left((\Gamma\check{\bar{\gamma}}_{ln})^2\right)\right]\left(\frac{\partial\check{u}}{\partial\check{r}}\right), \tag{5b}$$

$$\check{C}_{rz} = \mu_0\left[1 + \frac{m-1}{2}\left((\Gamma\check{\bar{\gamma}}_{ln})^2\right)\right]\left(\frac{\partial\check{w}}{\partial\check{r}} + \frac{\partial\check{u}}{\partial\check{z}}\right), \tag{5c}$$

$$\check{C}_{r\theta} = \mu_0\left[1 + \frac{m-1}{2}\left((\Gamma\check{\bar{\gamma}}_{ln})^2\right)\right]\left(\frac{\partial\check{v}}{\partial\check{r}} + \frac{1}{\check{r}}\frac{\partial\check{u}}{\partial\check{\theta}} - \frac{\check{v}}{\check{r}}\right), \tag{5d}$$

$$\check{C}_{\theta\theta} = \mu_0\left[1 + \frac{m-1}{2}\left((\Gamma\check{\bar{\gamma}}_{ln})^2\right)\right]\left(\frac{1}{\check{r}}\frac{\partial\check{v}}{\partial\check{\theta}} + \frac{\check{u}}{\check{r}}\right), \tag{5e}$$

$$\check{C}_{\theta z} = \mu_0\left[1 + \frac{m-1}{2}\left((\Gamma\check{\bar{\gamma}}_{ln})^2\right)\right]\left(\frac{1}{\check{r}}\frac{\partial\check{w}}{\partial\check{\theta}} + \frac{\partial\check{v}}{\partial\check{z}}\right), \tag{5f}$$

$$\check{C}_{zz} = \mu_0\left[1 + \frac{m-1}{2}\left((\Gamma\check{\bar{\gamma}}_{ln})^2\right)\right]\frac{\partial\check{w}}{\partial\check{z}}. \tag{5g}$$

Here, $u(r,\theta,z,t), v(r,\theta,z,t)$ and $w(r,\theta,z,t)$ represents the velocity components in r, θ *and* z directions respectively, p is the pressure, ρ is the density of bile and $\frac{\partial p}{\partial z}$ is the pressure gradient.

Assuming that the catheter is moving in the axial direction with velocity V_s and the catheter has a fixed radius r_s Porous boundary (Darcy) models transmural leakage/permeation through the duct wall (e.g., in a fistula or diseased epithelium) and aggregate epithelial hydraulic permeability and lymphatic uptake. Inclination captures the gravitational contribution relevant to anatomical placement. Suitable boundary conditions are as follows

$$u(r,\theta,z,t) = v(r,\theta,z,t) = 0 \; at \; r = R_w(z,t), \tag{6a}$$

$$-\frac{Knw}{\sqrt{Da}} = r_c\frac{\partial w}{\partial r} \; at \; r = R_w(z,t), \tag{6b}$$

$$w(r,\theta,z,t) = V_c \; at \; r = r_c. \tag{6c}$$

Assuming the system is at rest, i.e., no flow occurs.

$$u(r,\theta,z,t) = v(r,\theta,z,t) = w(r,\theta,z,t) = 0 \; at \; t = 0, \tag{6d}$$

Let us introduce non-dimensional variables

$$z = \frac{\check{z}}{L_0}, r = \frac{\check{r}}{R_0}, v = \frac{\check{v}}{c}, u = \frac{\lambda \check{u}}{cR_0}, \; \varepsilon = \frac{R_0}{l_0}, p = \frac{{R_0}^2 \check{p}}{L_0 \eta_0 c}, Re = \frac{\rho c R_0}{\mu_0}$$
$$t = \frac{c\check{t}}{l_0}, R(z) = \frac{R(\check{z})}{R_0}, \; H_w(z) = \frac{H_w(\check{z})}{R_0}, C_{zz} = \frac{L_0}{c\mu_o}\check{C}_{zz}, C_{rr} = \frac{R_0}{c\mu_o}\check{C}_{rr}, \quad \delta = \frac{R_0}{L_0}, \; We = \frac{c\Gamma}{R_0}, \check{\dot{\gamma}} = \frac{c\dot{\gamma}}{R_0} \tag{7}$$

Reduced non-dimensional equations are

$$\varepsilon\left[\frac{\partial u}{\partial r} + \frac{u}{r} + \frac{1}{r}\frac{\partial v}{\partial \theta}\right] + \frac{\partial w}{\partial z} = 0 \tag{8a}$$

$$Re\varepsilon^3\left(\frac{\partial u}{\partial t} + u\frac{\partial u}{\partial r} + \frac{v}{r}\frac{\partial u}{\partial \theta} - \frac{v^2}{r} + w\frac{\partial u}{\partial z}\right) = -\frac{\partial p}{\partial r} + \varepsilon\frac{1}{r}\frac{\partial}{\partial r}(rC_{rr}) + \varepsilon\frac{1}{r}\frac{\partial}{\partial \theta}(C_{r\theta}) + \varepsilon^2\frac{\partial}{\partial z}C_{rz} - \varepsilon\frac{C_{\theta\theta}}{r} - \frac{{R_0}^3\rho g}{L_0\mu_0 c}cos\alpha \tag{8b}$$

$$Re\varepsilon^3\left(\frac{\partial v}{\partial t} + u\frac{\partial v}{\partial r} + \frac{v}{r}\frac{\partial v}{\partial \theta} + \frac{uv}{r} + w\frac{\partial v}{\partial z}\right) = -\frac{1}{r}\frac{\partial p}{\partial \theta} + \varepsilon\frac{1}{r^2}\frac{\partial}{\partial r}(r^2C_{r\theta}) + \varepsilon\frac{1}{r}\frac{\partial}{\partial \theta}(C_{\theta\theta}) + \varepsilon^2\frac{\partial}{\partial z}C_{\theta z} \tag{8c}$$

$$Re\varepsilon\left(\frac{\partial w}{\partial t} + u\frac{\partial w}{\partial r} + \frac{v}{r}\frac{\partial w}{\partial \theta} + w\frac{\partial w}{\partial z}\right) = -\frac{\partial p}{\partial z} + \frac{1}{r}\frac{\partial}{\partial r}(rC_{rz}) + \frac{1}{r}\frac{\partial}{\partial \theta}(C_{\theta z}) + \varepsilon\frac{\partial}{\partial z}C_{zz} + \frac{{R_0}^2\rho g}{L_0\mu_0 c}sin\alpha \tag{8d}$$

Where $\eta = \frac{\rho g a^2}{\mu c}, \eta' = \frac{\rho g a^3}{\mu c \lambda}$, δ is the dimensionless wave number, We is the Weissenberg number, Re Reynolds number, and Kn Knudsen number.

The non-dimensional boundary conditions are

$$u(r,\theta,z,t) = v(r,\theta,z,t) = 0 \; at \; r = R_w(z,t), \tag{9a}$$

$$-\frac{Knw}{\sqrt{Da}} = r_s\frac{\partial w}{\partial r} at \; r = R_w(z,t) \tag{9b}$$

$$w(r,\theta,z,t) = V_c \; at \; r = r_c, \tag{9c}$$

Let the system be at rest, i.e., no flow takes place.

$$u(r,\theta,z,t) = v(r,\theta,z,t) = w(r,\theta,z,t) = 0 \; at \; t = 0, \tag{9d}$$

SOLUTION OF THE PROBLEM

Considering a steady and laminar bile flow in an eccentric tube under the lubrication approach by neglecting the higher-order terms of δ and Re. The equations of continuity, r-momentum, θ-momentum and z-momentum become

$$\frac{\partial p}{\partial r} = \eta' cos\alpha \tag{10a}$$

$$\frac{\partial p}{\partial z} - \eta sin\alpha = \frac{1}{r}\frac{\partial}{\partial r}(rC_{rz}) + \frac{1}{r}\frac{\partial}{\partial \theta}(C_{\theta z}) \tag{10b}$$

$$\frac{\partial p}{\partial \theta} = 0 \tag{10c}$$

$$C_{rz} = \left[1 + \frac{m-1}{2}We^2\left(\left(\frac{\partial w}{\partial r}\right)^2 + \left(\frac{1}{r}\frac{\partial w}{\partial \theta}\right)^2\right)\right]\left(\frac{\partial w}{\partial r}\right) \tag{10d}$$

$$C_{\theta z} = \mu_0\left[1 + \frac{m-1}{2}We^2\left(\left(\frac{\partial w}{\partial r}\right)^2 + \left(\frac{1}{r}\frac{\partial w}{\partial \theta}\right)^2\right)\right]\left(\frac{1}{r}\frac{\partial w}{\partial \theta}\right) \tag{10e}$$

We observe that equation (10b) cannot be solved analytically. The non-Newtonian behavior of bile is significant in small ducts at low shear rate, so we have assumed that the shear rate is low, i.e., $\Gamma\dot{\gamma} < 1$. Linearizing the equation in terms of the Weissenberg number We^2 by the regular perturbation technique.

$$w = w_0 + We^2 w_1 + \cdots,$$
$$p = p_0 + We^2 p_1 + \cdots,$$
$$q = q_0 + We^2 q_1 + \cdots, \tag{11}$$

Using equations (5a)-(5g) into equation (10b) we obtain:
Zeroth-order system of We^2 equations with boundary conditions

$$\frac{\partial^2 w_0}{\partial r^2} + \frac{1}{r}\frac{\partial w_0}{\partial r} = \frac{\partial p_0}{\partial z} - \eta sin\alpha \tag{12a}$$

$$-\frac{Knw_o}{\sqrt{Da}} = r_c\frac{\partial w_0}{\partial r}, \; at \; r = R_w(z,t), \; w_0 = V_c, \; at \; r = r_c, \tag{12b}$$

A first-order system of We^2 equations with boundary conditions

$$\frac{\partial^2 w_1}{\partial r^2}+\frac{1}{r}\frac{\partial w_1}{\partial r}=\frac{\partial p_1}{\partial z}-\frac{m-1}{2}\left(\frac{1}{r}\left(\frac{\partial w_0}{\partial r}\right)^3+\frac{\partial}{\partial r}\left(\frac{\partial w_0}{\partial r}\right)^3\right) \tag{12c}$$

$$w_0=O_c,\ at\ r=r_c,\ -\frac{Knw_1}{\sqrt{Da}}=r_c\frac{\partial w_1}{\partial r}\ \ at\ r=R_w(z,t) \tag{12d}$$

The slip boundary condition equation (12b), where Da is the Darcy number, which represents the porosity parameter, and Kn is the wall slip parameter, let $\chi=\frac{dp_0}{dz}-\eta sin\alpha$.
The solution of the zeroth-order system

$$w_0=\frac{1}{4}\chi r^2+A_{11}logr+A_{12} \tag{13a}$$

The solution of the first-order system

$$w_1=\frac{1}{4}\left(\frac{dp_1}{dz}\right)r^2-\frac{m-1}{2}\left[\frac{1}{32}(\chi)^3r^4-\frac{(A_{11})^3}{2r^2}+\frac{3}{8}(\chi)^2A_{11}r^2\right]+A_{13}logr+A_{14} \tag{6.13b}$$

The volumetric flow rate Q_o is given by

$$Q_o=\int_0^{R_w(z)}w_o r\mathrm{d}r=\int_0^{r_c}V_c r\mathrm{d}r+\int_{r_c}^{R_w(z)}w_o r\mathrm{d}r \tag{14a}$$

$$Q_o=V_c{r_c}^2+(\chi)\left(\frac{{R_w}^4-{r_c}^4}{8}\right)+A_{11}({R_w}^2\log\sqrt{R_w}-{r_c}^2log\sqrt{r_c})+A_{11}\left(\frac{{c_p}^2-{R_w}^2}{4}\right)+A_{12}\left(\frac{{R_w}^2-{r_c}^2}{2}\right) \tag{14b}$$

From equation (14b), we get

$$\frac{dp_0}{dz}=\left(\frac{8}{{R_w}^4-{r_c}^4}\right)\left(Q_o-V_c{r_c}^2-A_{11}({R_w}^2\log\sqrt{R_w}-{r_c}^2log\sqrt{r_c})-A_{11}\left(\frac{{r_c}^2-{R_w}^2}{4}\right)-A_{12}\left(\frac{{R_w}^2-{r_c}^2}{2}\right)\right)+\eta sin\alpha \tag{14c}$$

The volume flow rate Q_1 is given by

$$Q_1=\int_0^{R_w(z)}w_1 r\mathrm{d}r=\int_0^{r_c}O_c r\mathrm{d}r+\int_{r_c}^{R_w(z)}w_1 r\mathrm{d}r \tag{15a}$$

$$Q_1=\left(\frac{dp_1}{dz}\right)\left(\frac{{R_w}^4-{r_c}^4}{16}\right)-\frac{m-1}{2}\left[(\chi)^3\left(\frac{{R_w}^6-{r_c}^6}{192}\right)-\frac{(A_{11})^3}{2}log\left(\frac{R_w}{r_c}\right)+3(\chi)^2A_{11}\left(\frac{{R_w}^4-{r_c}^4}{32}\right)\right]$$
$$+A_{13}({R_w}^2\log\sqrt{R_w}-{r_c}^2log\sqrt{r_c})+A_{13}\left(\frac{{r_c}^2-{R_w}^2}{4}\right)+A_{14}\left(\frac{{R_w}^2-{r_c}^2}{2}\right) \tag{15b}$$

From equation (15b), we get

$$\frac{dp_1}{dz}=\left(\frac{16}{{R_w}^4-{r_c}^4}\right)\left(Q_1+\frac{m-1}{2}\left[(\chi)^3\left(\frac{{R_w}^6-{r_c}^6}{192}\right)-\frac{(A_{11})^3}{2}log\left(\frac{R_w}{r_c}\right)+3(\chi)^2A_{11}\left(\frac{{R_w}^4-{r_c}^4}{32}\right)\right]\right)$$
$$-\left(\frac{16}{{R_w}^4-{r_c}^4}\right)A_{13}({R_w}^2\log\sqrt{R_w}-{r_c}^2log\sqrt{r_c})-A_{13}\left(\frac{{r_c}^2-{R_w}^2}{4}\right)-A_{14}\left(\frac{{R_w}^2-{r_c}^2}{2}\right) \tag{15c}$$

Substituting in equation (11) we get

$$w=\frac{1}{4}(\chi)r^2+A_{11}logr+A_{12}+We^2\left\{\frac{1}{4}\left(\frac{dp_1}{dz}\right)r^2-\frac{m-1}{2}\left[\frac{1}{32}(\chi)^3r^4-\frac{(A_{11})^3}{2r^2}+\frac{3}{8}(\chi)^2A_{11}r^2\right]+A_{13}logr+A_{14}\right\} \tag{16a}$$

$$Q=V_c{r_c}^2+(\chi)\left(\frac{{R_w}^4-{r_c}^4}{8}\right)+A_{11}({R_w}^2\log\sqrt{R_w}-{r_c}^2log\sqrt{r_c})+A_{11}\left(\frac{{r_c}^2-{R_w}^2}{4}\right)+A_{12}\left(\frac{{R_w}^2-{r_c}^2}{2}\right)+$$
$$We^2\left\{\left(\frac{dp_1}{dz}\right)\left(\frac{{R_w}^4-{r_c}^4}{16}\right)-\frac{m-1}{2}\left[(\chi)^3\left(\frac{{R_w}^6-{r_c}^6}{192}\right)-\frac{(A_{11})^3}{2}log\left(\frac{R_w}{r_c}\right)+3(\chi)^2A_{11}\left(\frac{{R_w}^4-{r_c}^4}{32}\right)\right]\right\}$$
$$+We^2\left\{A_{13}({R_w}^2\log\sqrt{R_w}-{r_c}^2log\sqrt{r_c})+A_{13}\left(\frac{{r_c}^2-{R_w}^2}{4}\right)+A_{14}\left(\frac{{R_w}^2-{r_c}^2}{2}\right)\right\} \tag{16b}$$

Similarly,

$$\frac{dp}{dz}=\left(\frac{8}{{R_w}^4-{r_c}^4}\right)\left(Q_o-V_c{r_c}^2-A_{11}({R_w}^2\log\sqrt{R_w}-{r_c}^2log\sqrt{r_c})-A_{11}\left(\frac{{r_c}^2-{R_w}^2}{4}\right)-A_{12}\left(\frac{{R_w}^2-{r_c}^2}{2}\right)\right)+$$
$$\eta sin\alpha+We^2\left\{\left(\frac{16}{{R_w}^4-{r_c}^4}\right)\left(Q_1+\frac{m-1}{2}\left[(\chi)^3\left(\frac{{R_w}^6-{r_c}^6}{192}\right)-\frac{(A_{11})^3}{2}log\left(\frac{R_w}{r_c}\right)+3(\chi)^2A_{11}\left(\frac{{R_w}^4-{r_c}^4}{32}\right)\right]\right)\right\}$$

$$-We^2\left\{A_{13}({R_w}^2\log\sqrt{R_w}-{r_c}^2 log\sqrt{r_c})-A_{13}\left(\frac{{r_c}^2-{R_w}^2}{4}\right)-A_{14}\left(\frac{{R_w}^2-{r_c}^2}{2}\right)\right\} \quad (16c)$$

Where constants are

$$A_{11}=\left[4V_cKn+(\chi)\left(KnR_w{}^2-Knr_c{}^2+2\sqrt{Da}R_w{}^2\right)\right]\left(\frac{-1}{4\sqrt{Da}+Knlog\left(\frac{R_w}{r_c}\right)}\right)$$

$$A_{12}=V_c-\frac{1}{4}(\chi){r_c}^2-A_{11}\log r_c$$

$$A_{13}=\left(\frac{1}{\sqrt{Da}+Knlog\left(\frac{R_w}{r_c}\right)}\right)\left[\frac{1}{4}\frac{dp_1}{dz}\left(Knr_c{}^2-KnR_w{}^2-2\sqrt{Da}R_w{}^2\right)\right]+\left(\frac{1}{\sqrt{Da}+Knlog\left(\frac{R_w}{r_c}\right)}\right)\left(\frac{m-1}{2}\right)$$
$$\left\{(\chi)^3\frac{1}{32}\left(KnR_w{}^4-Knr_c{}^4+4\sqrt{Da}R_w{}^4\right)+16{A_{11}}^3+\frac{3A_{11}}{8}(\chi)^2\left(KnR_w{}^2-Knr_c{}^2+2\sqrt{Da}R_w{}^2\right)\right\}$$
$$+\left(\frac{1}{\sqrt{Da}+Knlog\left(\frac{R_w}{r_c}\right)}\right)\left(\frac{m-1}{2}\right)\frac{{A_{11}}^3}{2}\frac{\left(KnR_w{}^2-Knr_c{}^2+2\sqrt{Da}r_c{}^2\right)}{R_w{}^2r_c{}^2}$$

$$A_{14}=-A_{13}logr_c-\frac{r_c{}^2}{4}\frac{dp_1}{dz}+\left(\frac{m-1}{2}\right)\left\{\frac{r_c{}^4}{32}(\chi)^3-\frac{{A_{11}}^3}{2r_c{}^2}+\frac{3A_{11}r_c{}^2}{8}(\chi)^2\right\}$$

RESULTS AND DISCUSSION

In the present paper, the effect of various physiological parameters involved in the peristaltic flow of bile in an inclined eccentric tube filled with a porous medium is analyzed. The results of the present mathematical model are evaluated with the help of MATLAB 2021a. The range of physiological parameters to analyze the resulting expressions of axial velocity w, and pressure gradient $\frac{dp}{dz}$ and the volumetric flow rate Q in this study, the porosity parameter Da, angle of inclination α, Weissenberg number We, velocity of the catheter V_c, radius of catheter r_c, gravity parameter η, wall slip parameter Kn and fluid behavior index m.

The axial velocity profile with respect to radial distance has been made from Figures 2(a)–2(h) for several values to emerging parameters and the graphs shows that the axial velocity is maximum at the surface of the catheter (outer wall of catheter) and as we move towards the wall of duct axial velocity decreases and is minimum at the wall. Figure 2(a) shows the effect of the porosity parameter on axial velocity. The axial velocity increases with the porosity parameter; maximum velocity occurs at the highest value of porosity parameter because the number of pores increases with the increase of porosity parameter, so the fluid can easily move through the duct. In Figure 2(b), we see the effect of the angle of inclination on axial velocity. The axial velocity increases with the increase in angle of inclination. An inclined duct helps to pass fluid quickly through the duct, so inclination marks a positive impact on axial velocity. In Figure 2(c), we observe that the axial velocity falls as we increase the Weissenberg number. The high elasticity of fluid reduces the axial velocity. Figure 2(d) displays the axial velocity profile for different values of the radius of the catheter. It is noticed that axial velocity increases with the increase in catheter radius. In Figure 2(e), we see that the axial velocity increases with the velocity of the catheter and is justified by the nature of the curve. If we increase the velocity of the catheter, it helps to raise the velocity of the fluid. Figure 2(f) shows the effect of the gravity parameter on axial velocity. The axial velocity increases with the gravity parameter, because the bile flows from the upper body parts to the lower parts of the body, so gravity plays an important role in flow. In Figure 2(g), we see that the axial velocity falls with wall slip conditions as it produces a hindrance to flow at the duct wall of the duct, so velocity reduces for a higher wall slip parameter. Figure 2(h) shows the effect of fluid behavior index on axial velocity for large values of m . The fluid is in the shear-thinning condition and at $m = 1$. Fluid behaves like a Newtonian fluid, clearly showing axial velocity increases with the fluid behavior index.

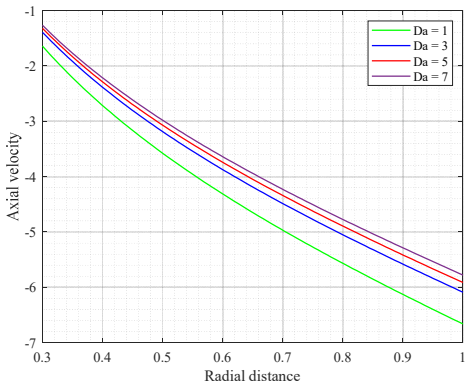

Figure 2(a). Profile of axial velocity w with r for different values of Da with $\alpha=\frac{\pi}{4}, We=3, r_c=0.15, V_c=0.25, \eta=0.35, Kn=0.2, b=0.5, m=0.3685$

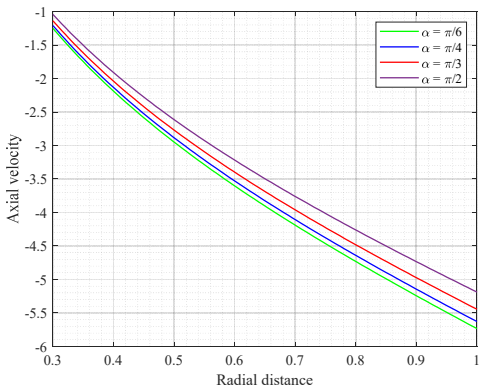

Figure 2(b). Profile of axial velocity w with r for different values of α with $Da=3, We=3, r_c=0.15, V_c=0.25, \eta=0.35, Kn=0.2, b=0.5, m=0.3685$

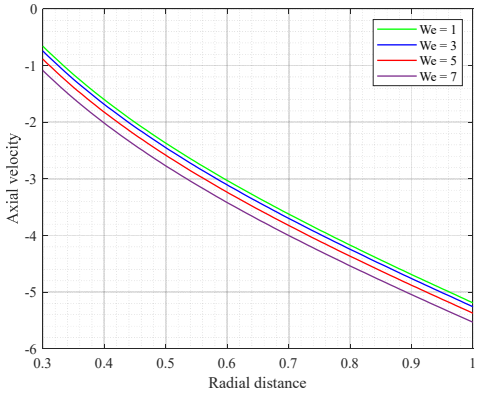

Figure 2(c). Profile of axial velocity w with r for different values of We with $Da = 3, \alpha = \frac{\pi}{4}, r_c = 0.15, V_c = 0.25, \eta = 0.35, Kn = 0.2, b = 0.5, m = 0.3685$

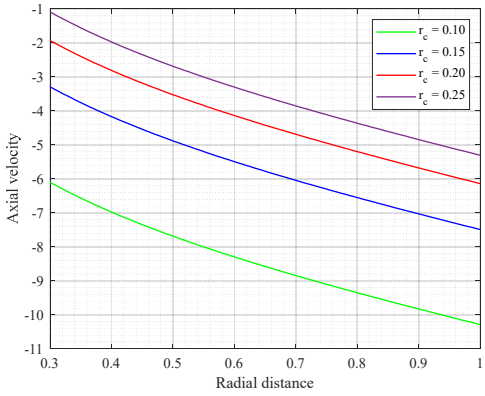

Figure 2(d). Profile of axial velocity w with r for different values of r_c with $Da = 3, \alpha = \frac{\pi}{4}, We = 3, V_c = 0.25, \eta = 0.35, Kn = 0.2, b = 0.5, m = 0.3685$

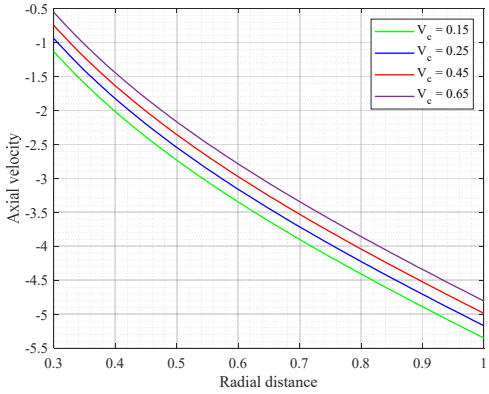

Figure 2(e). Profile of axial velocity w with r for different values of V_p with $Da = 3, \alpha = \frac{\pi}{4}, We = 3, r_c = 0.15, \eta = 0.35, Kn = 0.2, b = 0.5, m = 0.3685$

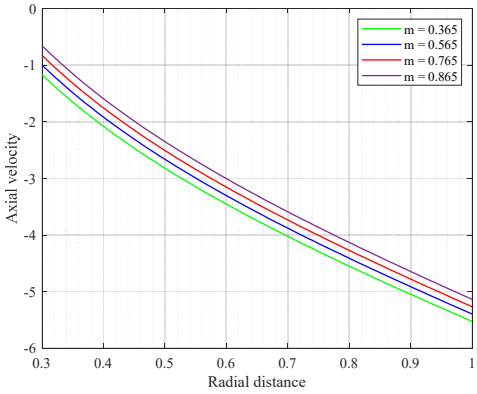

Figure 2(h). Profile of axial velocity w with r for different values of, m with $Da = 3, \alpha = \frac{\pi}{4}, We = 3, r_c = 0.15 V_c = 0.25, \eta = 0.35, Kn = 0.2, b = 0.5$

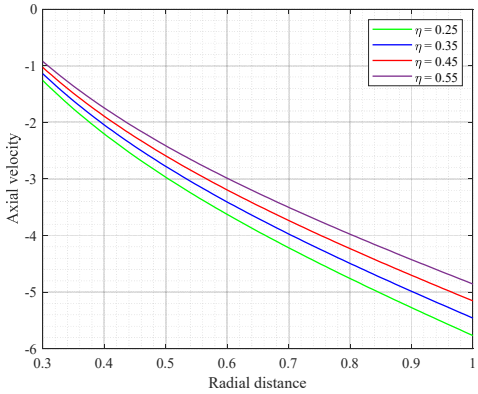

Figure 2(f). Profile of axial velocity w with r for different values of η with $Da = 3, \alpha = \frac{\pi}{4}, We = 3, V_c = 0.25\, r_c = 0.15, Kn = 0.2, b = 0.5, m = 0.3685$

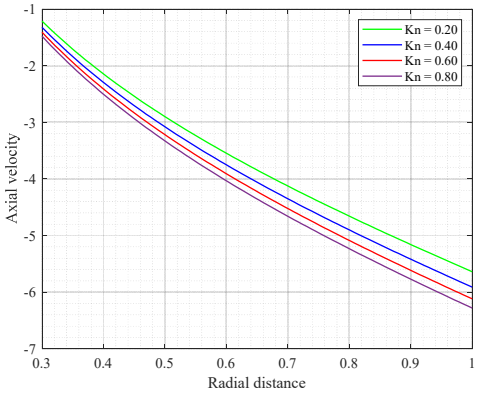

Figure 2(g). Profile of axial velocity w with r for different values of Kn with $Da = 3, \alpha = \frac{\pi}{4}, We = 3, r_c = 0.15, \eta = 0.35, V_c = 0.25, b = 0.5, m = 0.3685$

Figures 3(a)–3(h) show pressure gradient distributions with respect to the axial distance of the various emerging parameters, and the graphs depict that more pressure is required to maintain the same flux in the narrow part of the duct due to the flexible wall, the duct contract or expand along the z-axis. Figure 3(a) shows the effect of the porosity parameter on the pressure gradient. The pressure decreases with increasing the porosity parameter. The minimum pressure is required to maintain the same flow rate at high porosity parameters, because porosity directly signifies the number of pores in a porous medium, so fluid passes easily through a porous duct for a high value of porosity parameter. Figure 3(b) shows the effect of angle of inclination on pressure gradient and observed that a lower pressure is required to maintain the same flux at a more inclined duct, i.e., the pressure gradient falls as we raise the value of inclination. Figure 3(c) shows the effect of Weissenberg number on the pressure gradient. More pressure is required to maintain the constant flux for an elastic fluid. Pressure gradient increases as we raise the Weissenberg number. In Figure 3(d), we see that low

pressure is required to pass through the duct with a large size of radius of the catheter, clearly indicating that the pressure decreases as we increase the radius of the catheter. Figure 3(e) shows that pressure reduces as the velocity of the catheter increases; the high catheter velocity helps in maintaining the flow so that the fluid can easily move in the duct. In Figure 3(f), we observe that the pressure gradient drops as the value of the gravity parameter increases. Figure 3(g) displays the pressure gradient distribution for distinct values of the wall slip parameter, as the wall slip parameter increases value of pressure also increases. The wall slip parameter shows a negative impact on the flow. In Figure 3(h), we see the effect of fluid behavior index on the pressure gradient. The low pressure is needed to maintain the same flow rate with the increment in the value of the fluid behavior index.

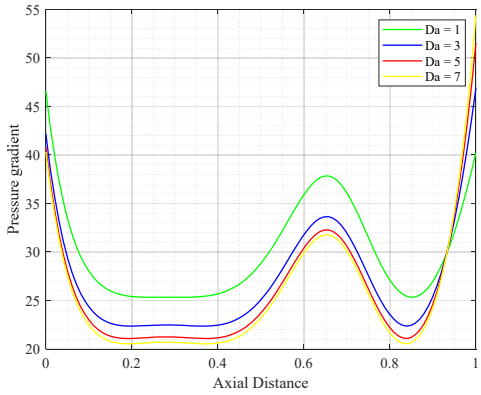

Figure 3(a). Profile of pressure gradient $\frac{dp}{dz}$ with z for different values of Da with $\alpha = \frac{\pi}{4}, We = 3, r_c = 0.15, V_c = 0.25, \eta = 0.35, Kn = 0.2, b = 0.5, m = 0.3685$

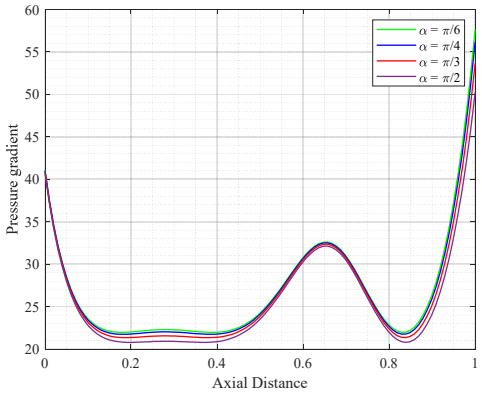

Figure 3(b). Profile of pressure gradient $\frac{dp}{dz}$ with z for different values of α with $Da = 3, We = 3, r_c = 0.15, V_c = 0.25, \eta = 0.35, Kn = 0.2, b = 0.5, m = 0.3685$

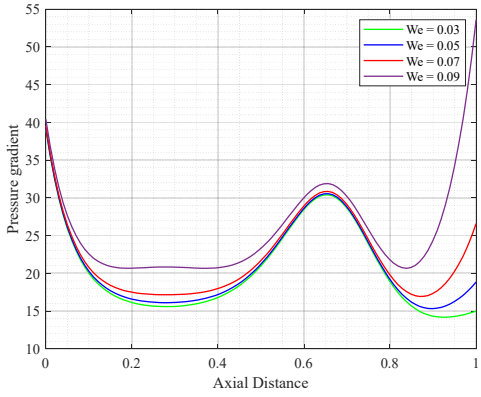

Figure 3(c). Profile of pressure gradient $\frac{dp}{dz}$ with z for different values of We with $Da = 3, \alpha = \frac{\pi}{4}, r_c = 0.15, V_c = 0.25, \eta = 0.35, Kn = 0.2, b = 0.5, m = 0.3685$

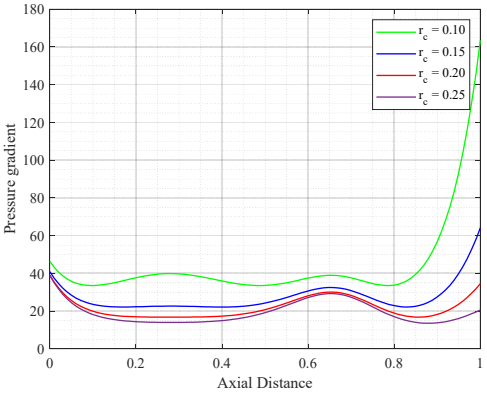

Figure 3(d). Profile of pressure gradient $\frac{dp}{dz}$ with z for different values of r_c with $Da = 3, \alpha = \frac{\pi}{4}, We = 3, V_c = 0.25, \eta = 0.35, Kn = 0.2, b = 0.5, m = 0.3685$

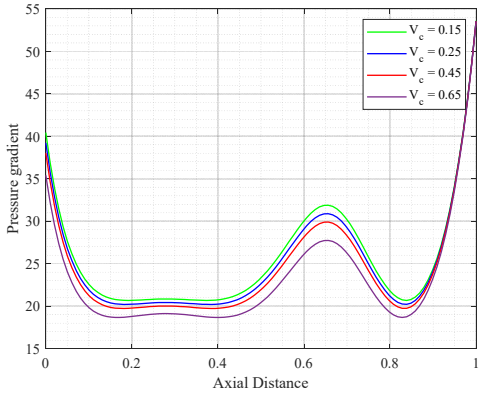

Figure 3(e). Profile of pressure gradient $\frac{dp}{dz}$ with z for different values of V_c with $Da = 3, \alpha = \frac{\pi}{4}, We = 3, r_c = 0.15, \eta = 0.35, Kn = 0.2, b = 0.5, m = 0.3685$

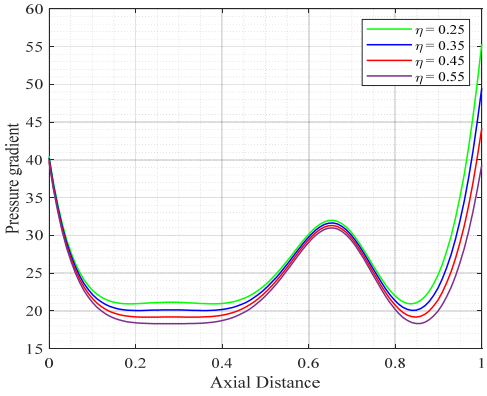

Figure 3(f). Profile of pressure gradient $\frac{dp}{dz}$ with z for different values of η with $Da = 3, \alpha = \frac{\pi}{4}, We = 3, V_c = 0.25\ r_c = 0.15, Kn = 0.2, b = 0.5, m = 0.3685$

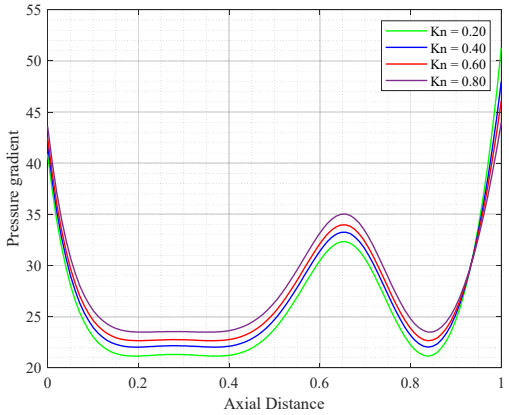

Figure 3(g). Profile of pressure gradient $\frac{dp}{dz}$ with z for different values of Kn with $Da = 3,\ \alpha = \frac{\pi}{4}, We = 3\ , r_c = 0.15\ , \eta = 0.35, V_c = 0.25, b = 0.5, m = 0.3685$

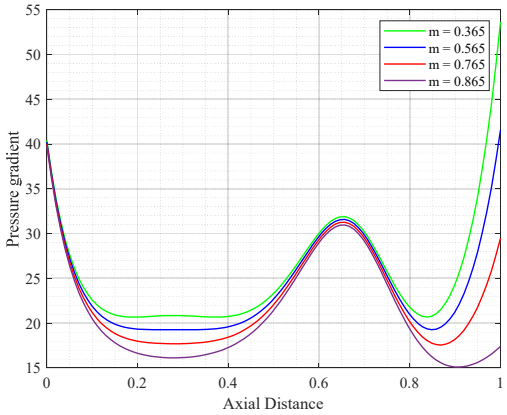

Figure 3(h). Profile of pressure gradient $\frac{dp}{dz}$ with z for different values of, m with $Da = 3,\ \alpha = \frac{\pi}{4}, We = 3\ , r_c = 0.15\ V_c = 0.25, \eta = 0.35, Kn = 0.2, b = 0.5$

Figures 4(a)–4(h) display the flow rate concerning axial distance for numerous values of decisive parameters. The nature of the curves is the same along the z-axis; maximum flow occurs when the duct is expanded. Figure 4(a) shows the effect of the porosity parameter on the flow rate. The flow rate increases with the porosity parameter because the number of pores increases, which leads to flow rate. In Figure 4(b), we observe that the flow rate enhances with the angle of inclination. The flow of fluid is downwards, so inclination increases the flow rate. In Figure 4(c), we see that the flow rate decreases with Weissenberg number, which means a high elastic fluid will not be able to pass easily through the eccentric duct. An increase in the Weissenberg number (We) and the wall slip parameter (Kn) leads to a decrease in bile flow velocity because of the Weissenberg number (elasticity). The Weissenberg number measures the relative importance of elastic stresses to viscous stresses (We = λU/L). In a Carreau fluid, higher We implies stronger viscoelastic effects. Elastic normal stresses generated within the fluid resist deformation and act as an additional resistance to the pressure-driven flow. As a result, for the same driving pressure gradient, the axial velocity decreases because part of the input energy is stored elastically rather than converted into forward motion. Similar behavior has been reported in peristaltic transport of Carreau fluids in eccentric tubes, where velocity decreases with We (Nadeem et al., [8]; Reima et al., [11]). In Figure 4(d), we see that the flow rate falls as the radius of the catheter increases. It means maximum fluid passes through the inner tube with fixed velocity, and the rest of the fluid moves through the porous duct. In Figure 4(e), we observe that the flow increases with the increase in catheter velocity. The fluid is passed quickly through the catheter. Figure 4(f) shows the effect of the gravity parameter on flow rate, indicating clearly that the gravity parameter has a positive impact on the flow rate. From Figure 4(g), we noticed that the flow rate reduces with the wall slip parameter. Figure 4(h) displays the effect of fluid behavior index on flow rate. The flow rate increases as we increase the value of m, as the value of the fluid behavior index tends to 1, the flow rate increases.

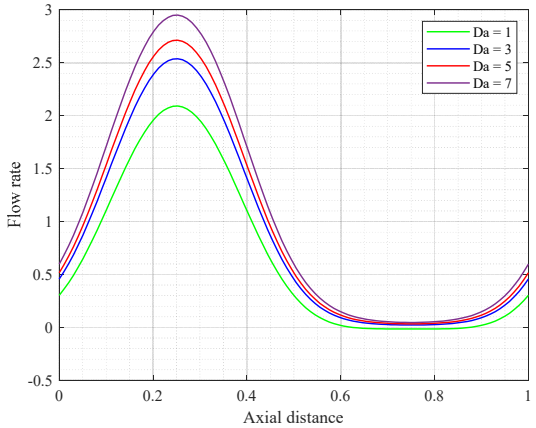

Figure 4(a). Profile of flow rate Q with z for different values of Da with $\alpha = \frac{\pi}{4}, We = 3\ , r_c = 0.15, V_c = 0.25\ , \eta = 0.35, Kn = 0.2, b = 0.5, m = 0.3685$

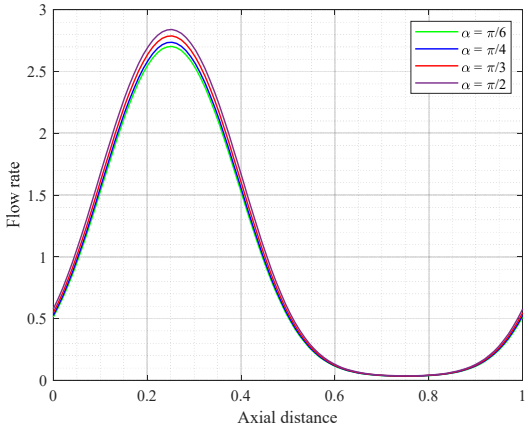

Figure 4(b). Profile of flow rate Q with z for different values of α with $Da = 3, We = 3\ , r_c = 0.15, V_c = 0.25\ , \eta = 0.35, Kn = 0.2, b = 0.5, m = 0.3685$

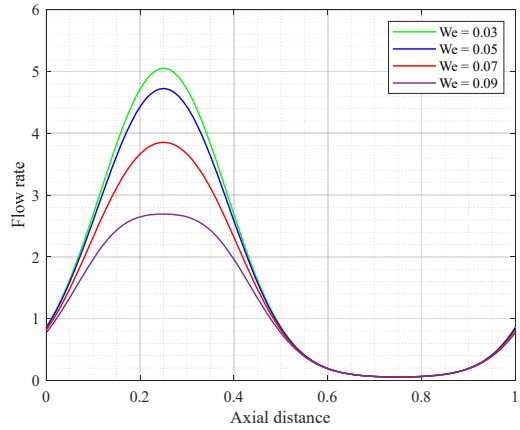

Figure 4(c). Profile of flow rate Q with z for different values of We with $Da = 3, \alpha = \frac{\pi}{4}, r_c = 0.15, V_c = 0.25, \eta = 0.35, Kn = 0.2, b = 0.5, m = 0.3685$

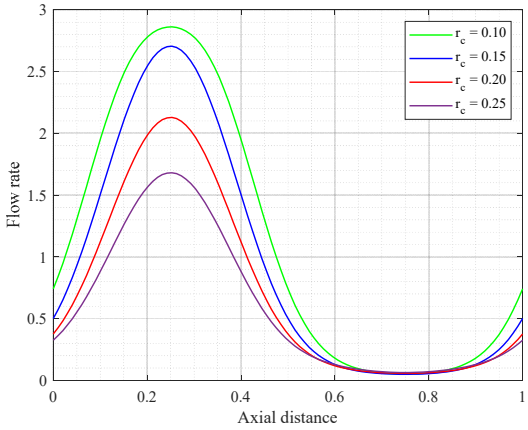

Figure 4(d). Profile of flow rate Q with z for different values of r_c with $Da = 3, \alpha = \frac{\pi}{4}, We = 3, V_c = 0.25, \eta = 0.35, Kn = 0.2, b = 0.5, m = 0.3685$

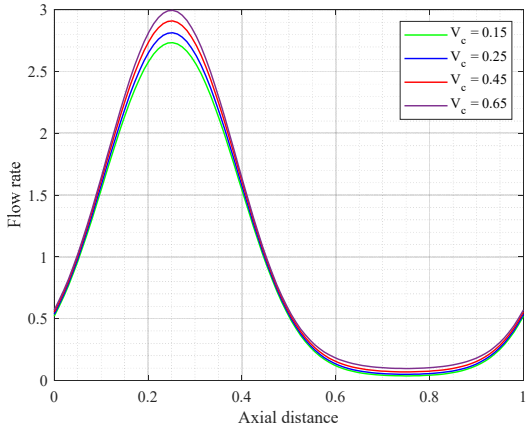

Figure 4(e). Profile of flow rate Q with z for different values of V_c with $Da = 3, \alpha = \frac{\pi}{4}, We = 3, r_c = 0.15, \eta = 0.35, Kn = 0.2, b = 0.5, m = 0.3685$

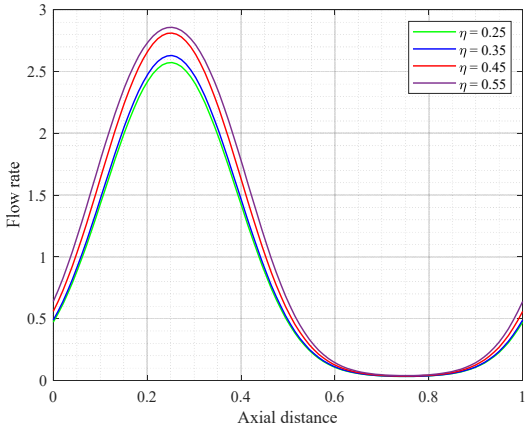

Figure 4(f). Profile of flow rate Q with z for different values of η with $Da = 3, \alpha = \frac{\pi}{4}, We = 3, V_c = 0.25\ r_c = 0.15, Kn = 0.2, b = 0.5, m = 0.3685$

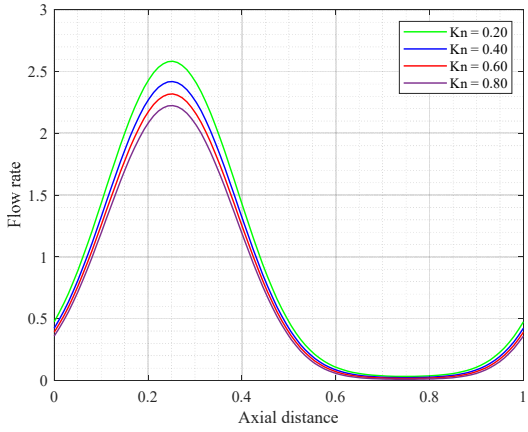

Figure 4(g). Profile of flow rate Q with z for different values of Kn with $Da = 3, \alpha = \frac{\pi}{4}, We = 3, r_c = 0.15, \eta = 0.35, V_c = 0.25, b = 0.5, m = 0.3685$

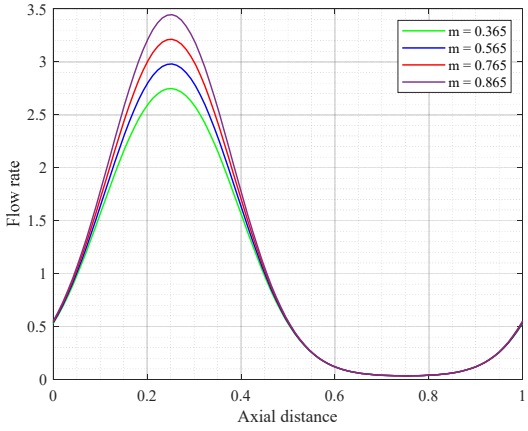

Figure 4(h). Profile of flow rate Q with z for different values of, m with $Da = 3, \alpha = \frac{\pi}{4}, We = 3, r_c = 0.15\ V_c = 0.25, \eta = 0.35, Kn = 0.2, b = 0.5$

This discussion is consistent with representative studies (Nadeem et al. [8]; Reima et al. [11]) that report similar trends in velocity, shear, and flow rate with elasticity and catheterization. Reduction in axial velocity with increased elasticity and changes with catheter radius are consistent with previous Carreau/eccentric-catheter studies. The standard values of the parameters shown in the discussion are based on referenced or experimentally verified. These parameters correspond to the realistic situations.

CONCLUSIONS

The bile is considered a non-Newtonian fluid. A comprehensive perturbation resolution has been discovered for Carreau fluid flow down an inclined eccentric catheterized duct with a porous wall containing bile. The obtained results in the case of Carreau fluid reveal that the flow characteristics are dependent on many parameters, such as catheter radius, catheter velocity, angle of inclination, gravity parameter, porosity parameter, Weissenberg number, fluid behavior index, and wall slip parameter. The key conclusions based on trends observed in the graphs are given as:

- Axial velocity and flow rate increase with an increased catheter velocity, angle of inclination, gravity parameter, porosity parameter, and fluid behavior index. It shows the positive impact on velocity and flux, which helps to move bile through the duct. Increase in axial velocity and flow rate at higher Darcy numbers in our simulations reflects that a more porous wall reduces resistance to flow, with clinical observations that bile escapes more readily when the duct wall loses its tight barrier function.
- Axial velocity and flow rate show a reverse nature with an increased Weissenberg number and wall slip parameter.
- Axial velocity is maximum at the outer surface of the catheter and is minimum at the wall of the duct.
- A catheter with a small radius increases the flow of bile. If the catheter size is large, it reduces the flow rate.
- In case of pressure gradient, more pressure is required to maintain the same flux with higher values of Weissenberg number, and for other parameters, low pressure is required to maintain the same flux.
- The reduction in wall shear stress due to shear-thinning also agrees with rheological observations of bile. Kuchumov et al. [5] analyzed the results of experiments, which relate well to the quantitative outcomes for bile. The present study is limited to theoretical outcomes considering the experimentally validated data. Even this analysis needs to be compared with clinical data in future work.

Acknowledgement

This research project was funded by the University of Technology and Applied Sciences, Shinas, through the Internal Research Funding Program-2025, grant number (UTAS-Shinas-cy02-2025-005).

The authors are grateful to Prof. S.P. Singh, Department of Mathematics, Dayalbagh Educational Institute, Agra, Uttar Pradesh (India), for his valuable guidance and support in conducting this research.

Conflict of Interests

There is no conflict of interest.

Data Availability Statement

The data will be made available on request.

Consent to Participate

There is no participation or involvement of any human/animal in this research article.

ORCID

Devendra Kumar, https://orcid.org/0000-0002-2346-8445; **Tanuj Kumar Rawat,** https://orcid.org/0009-0006-5907-1825
Mahesh Garvandha, https://orcid.org/0000-0002-4751-5840; **Sudhakar Kumar Chaubey,** https://orcid.org/0000-0002-3882-4596

REFERENCES

[1] W. Cao, M.M. Kaleem, M. Usman, M. Imran Asjad, M.Y. Almusawa, and S.M. Eldin, "A study of fractional Oldroyd-B fluid between two coaxial cylinders containing gold nanoparticles," Case Studies in Thermal Engineering, **45**, 102949 (2023). https://doi.org/10.1016/j.csite.2023.102949

[2] M. Dhange, G. Sankad, R. Safdar, W. Jamshed, M.R. Eid, U. Bhujakkanavar, S. Gouadri, and R. Chouikh, "A mathematical model of blood flow in a stenosed artery with post-stenotic dilatation and a forced field," Plos one, **17**(7), e0266727 (2022). https://doi.org/10.1371/journal.pone.0266727

[3] M. Gudekote and R. Choudhari, "Slip Effects on Peristaltic Transport of Casson Fluid in an Inclined Elastic Tube with Porous Walls," Journal of Advanced Research in Fluid Mechanics and Thermal Sciences, **43**(1), 67–80 (2018).

[4] J.W. Ostroff, J.P. Roberts, R.L. Gordon, R.L., E.J. Ring, and N.L. Ascher, "The management of T tube leaks in orthotopic liver transplant recipients with endoscopically placed nasobiliary catheters," Transplantation, **49**(5), 922-924 (1990). https://doi.org/10.1097/00007890-199005000-00018

[5] A.G. Kuchumov, Y.L. Nyashin, V.A. Samartsev, "Modeling of Peristaltic Bile Flow in the Papilla Ampoule with Stone and in the Papillary Stenosis Case: Application to Reflux Investigation," in: *7th WACBE World Congress on Bioengineering, IFMBE Proceedings,* edited by J. Goh, and C. Lim, vol. **52**, (Springer, Cham. 2015). https://doi.org/10.1007/978-3-319-19452-3_42

[6] L.B. McCash, S. Akhtar, S. Nadeem, S. Saleem, and A. Issakhov, "Viscous flow between two sinusoidally deforming curved concentric tubes: advances in endoscopy," Science Report, **11**, 15124 (2021). https://doi.org/10.1038/s41598-021-94682-8

[7] N.T. Eldabe, M.Y. Abouzeid, and H.A. Ali, "Effect of Heat and Mass Transfer on Casson Fluid Flow Between Two Co-Axial Tubes with Peristalsis," Journal of Advanced Research in Fluid Mechanics and Thermal Sciences, **76**, 54-75 (2020). https://doi.org/10.37934/arfmts.76.1.5475

[8] S. Nadeem, A. Riaz, R. Ellahi, and N.S. Akbar, "Series solution of unsteady peristaltic flow of a Carreau fluid in eccentric cylinders," Ain Shams Engineering Journal, **5**, 293–304 (2014). https://doi.org/10.1016/j.asej.2013.09.005

[9] S.M. Nurulaifa, Z. Ismail, and N.A. Jaafar, "Mathematical Modeling of Unsteady Solute Dispersion in Bingham Fluid Model of Blood Flow Through an Overlapping Stenosed Artery," Journal of Advanced Research in Fluid Mechanics and Thermal Sciences, **87**, 134-147 (2021). https://doi.org/10.37934/arfmts.87.3.134147

[10] Q. Raza, X. Wang, M.Z. Qureshi, S.M. Eldin, A.A. Allah, B. Ali, and I. Siddique, "Mathematical modeling of nanolayer on biological fluids flow through porous surfaces in the presence of CNT," Case Studies in Thermal Engineering, **45**, 102958 (2023). https://doi.org/10.1016/j.csite.2023.102958
[11] R.D. Alsemiry, H.M. Sayed, and N. Amin, "Mathematical analysis of Carreau fluid and heat transfer within an eccentric catheterized artery," Alexandria Engineering Journal, **61**, 523–539 (2022). https://doi.org/10.1016/j.aej.2021.06.029
[12] T. Sauerbruch, M. Weinzierl, J. Holl, and E. Pratschke, "Treatment of Postoperative Bile Fistulas by Internal Endoscopic Biliary Drainage," Gastroenterology, **90**(6), 1998-2003 (1986). https://doi.org/10.1016/0016-5085(86)90273-8
[13] S.M. Strasberg, C.N. Petrunka, R.G. Ilson, and J.E. Paloheimo, "Characteristics of Inert Solute Clearance by the Monkey Liver," Gastroenterology, **76**(2), 259-266 (1978). https://doi.org/10.1016/0016-5085(79)90331-7
[14] D. Tripathi, "Study of transient peristaltic heat flow through a finite porous channel," Mathematical and Computer Modeling, **57**, 1270-1283 (2013). https://doi.org/10.1016/j.mcm.2012.10.030

ПЕРИСТАЛЬТИЧНИЙ ПОТІК ЖОВЧІ В АМПУЛІ СОСОЧКА З ПОРИСТИМИ СТІНКАМИ ТА ПОХИЛОЮ ЕКЦЕНТРИЧНОЮ КАТЕТЕРИЗОВАНОЮ ПРОТОКОЮ

Д. Кумар[1], Т.К. Рават[2], М. Гарванда[1], С. Кумар[3], С.К. Чаубей[1]

[1]*Відділ наук та математики, кафедра допоміжних вимог, університет технологій та прикладних наук-Шинас, Оман*
[2]*Університет GLA, Велика Нойда, Індія*
[3]*Університет доктора Бхімрао Амбедкара, Агра, Індія*

У цьому дослідженні математично досліджується комбінований вплив нахилу та катетера на біліарний потік рідини Карро через ексцентричну катетеризовану протоку з пористим матеріалом. Технічне збурення використовується для розв'язання керівних рівнянь, враховуючи низькі числа Рейнольдса, довгохвильове наближення та відповідні малі параметри. Хірургічна техніка, коли катетер ексцентрично вводиться в протоку, пов'язана з результатами дослідження. Для досягнення аналітичних рішень було використано кілька параметрів. У цих даних відображаються осьова швидкість, градієнт тиску, швидкість потоку та напруга зсуву стінки, а також такі нові параметри: параметр ковзання стінки, число Вайсенберга, індекс поведінки рідини, число Дарсі та кут нахилу. Градієнт тиску значно змінюється кутом нахилу та параметром пористості, а осьова швидкість катетера падає зі збільшенням числа Вайсенберга. Фізіологічні спостереження узгоджуються з цими висновками.

Ключові слова: *перистальтичний потік жовчі; цибулина сосочка; пористі стінки; похила ексцентрична катетеризована протока*